

Performance analysis of single-phase interior permanent magnet synchronous motor

Benjamin Olabisi Akinloye¹, Emeka Simon Obe²

¹Department of Electrical and Electronics Engineering, Federal University of Petroleum Resources, Effurun, Nigeria

²Department of Electrical Engineering, University of Nigeria, Nsukka, Nigeria

Article Info

Article history:

Received Aug 15, 2021

Revised Mar 19, 2022

Accepted Apr 5, 2022

Keywords:

Auxiliary winding

d-q analysis

Main winding

Single-phase

Symmetrical components

ABSTRACT

Single-phase permanent magnet synchronous motor has been tipped as an alternative to single-phase induction motor due to its high efficiency and torque density. Consequently, a proper performance analysis of the motor is required to cope with the stator imbalance in order to prevent pulsation in the torque performance. This paper presented the dynamic and steady-state analysis of a single-phase interior permanent magnet synchronous motor. In this analysis, a proper combination of direct-quadrature (d-q) reference frame, and symmetrical component analyses were used. The symmetrical components analysis was used to obtain the steady state performance while the dynamic performance was obtained from d-q analysis. The symmetrical components cope with the imbalance and hence the resulting torque pulsation which may results in heating of the motor. The results obtained agreed with the theoretical analysis and yielded a unique steady state equivalent circuit and phasor diagram. The models of the motor were simulated using MATLAB/Simulink. A prototype of the motor was developed and experimentation was carried out to validate the dynamic performance.

This is an open access article under the [CC BY-SA](https://creativecommons.org/licenses/by-sa/4.0/) license.



Corresponding Author:

Benjamin Olabisi Akinloye

Department of Electrical and Electronics Engineering, Federal University of Petroleum Resources

East/West Road, Effurun, Delta State, Nigeria

Email: akinloye.benjamin@fupre.edu.ng

1. INTRODUCTION

Permanent magnet machine is made by replacing the winding in the rotor of a synchronous machine by a strong permanent magnet [1]. Permanent magnet synchronous motors have so many rotor types, some of which are surface magnet rotor, inset magnet rotor, and interior magnet rotor [2]. The interior magnet rotor can be of single- or double-layer permanent magnet (PM). The number of layers of PM in the rotor of permanent magnet synchronous motor is limited by the rotor dimension and the effect of saturation. The interest in single-phase permanent magnet synchronous motor (SPIPMSM) has rapidly increased for both domestic and industrial purpose [2], [3]. The chronological advancement of researches on SPIPMSM was put to paper by [4]. d-q axis theory was used to demonstrate both the dynamic and steady state performance analysis of SPIPMSM [4]. This method neglected the imbalance in the stator windings of the motor but acknowledged the efficiency of SPIPMSM as compared to single-phase induction motor. The level of efficiency in electric motor has been raised to a level that improvement on induction motor may not achieve [3]–[6]. Therefore, it becomes imperative to carry out further research on the motor in order to improve the working performance.

The single-phase interior permanent magnet synchronous motor, just like single-phase induction motor, operates like a two phase motor with main, and auxiliary winding have different number of turns [7]–

[9]. From mid-20th century, various methods were developed for both steady, and dynamic state analysis of permanent magnet synchronous motor [8]–[10]. These methods were mostly designed for polyphase permanent magnet synchronous motor and few papers focused on the single-phase counterpart of this motor. Performance analysis of SPIPMSM cannot be carried out with the same models developed for the polyphase motors due to the presence of imbalance experienced by its stator [11]. Few authors [7], [11]–[15] that focus on the single phase type of the motor seldom venture into the detail mathematical models or use assumptions of lumped parameters [16] which in turns impair the quality of the performance of the motor. This paper presents a detailed modelling of SPIPMSM using d-q analytical technics for the dynamic performance and symmetrical component analysis for the steady-state performance. The starting capacity of single-phase line start permanent magnet motor was enhanced by [17] using the tapered air-gap of the motor to overcome the starting limitation. The imbalance experience by the motor still remains even if the starting capacity is enhanced. The dimension of PM and its position in the rotor was optimized by [18]–[20] using Taguchi method. The high effectiveness of SPIPMSM has attracted its usage in the power system industry for high voltage breaker system [21]. Experiments and simulations were performed to improve the efficiency of permanent magnet synchronous motor in [22]. Kurihara *et al.* [23] discussed the trade-off that must be made between starting capability and efficiency. For efficiency to improve for single-phase PMSM, there must be a trade-off of the starting capability. Experimental method was used to demonstrate the trade-off in the number of turns of main winding to that of auxiliary winding. The single-phase loading of an isolated three phase PM synchronous generator was considered by [24] and the single-phase characteristics with consideration of various power factors was presented in [25].

Modified output equation was used in [26] to design fractional horsepower PMSM. The design was analysed using Ansys Maxwell two-dimensional (2D). In addition, the same method of Ansys Maxwell 2D was used in the design and efficiency improvement of single-phase induction motor in [27]–[31]. The designed motor in [26] proved to have a higher efficiency than the induction motor it was to replace. Chang in [32] presented an analysis of unexcited synchronous motors. The single-phase reluctance synchronous motor was the focus of the work. Derivation of equivalent circuit of single-phase permanent magnet synchronous motor was presented in [33].

Both [32] and [33] employed the method of double revolving field theory to obtain the equivalent circuits of the motors for steady state. This work further the work done in [32] and [33] by using method of symmetrical component analysis to obtain both steady state equivalent circuit and the phasor diagram. Symmetrical components analysis copes with the imbalance in the stator and hence reduces the torque pulsation that might results in heating of the motor. The models in the present work are detailed breaking down the rigorous mathematical equations involved in the analysis. The present work also presents results which clearly show the effects of negative and positive sequence in the steady-state performance of SPIPMSM by using symmetrical components analysis.

2. METHOD OF ANALYSIS

In order to create a rotating magnetic field for single-phase interior permanent magnet synchronous motor, the stator must be constructed with a split-phase (main and auxiliary winding). The angle between these windings may vary. A capacitor is connected in series with the auxiliary winding so that the auxiliary current will lead the main current to create a rotating field.

2.1. Dynamic performance analysis

The analysis of the motor under study starts with the equation of the machine in the d-q reference frame. Figure 1 shows the circuit connection of main and auxiliary winding of SPIPMSM with starting and running capacitors. In order to investigate the dynamic performance of SPIPMSM, the work neglects saturation and assumes the windings have the same turn ratios. It does not consider the PM in the rotor and neglects eddy current and hysteresis losses. The axes of transformation into d-q axes are shown in Figure 2.

Let v_m and v_a be the instantaneous stator voltages of both main and auxiliary windings, r_m and r_a are the main and auxiliary winding resistance, λ_m and λ_a are flux linking main and auxiliary winding:

$$v_{ms} = r_m i_{ms} + p\lambda_{ms} \quad (1)$$

$$v_{as} - v_c = r_a i_{as} + p\lambda_{as} \quad (2)$$

where

$$v_c = \frac{1}{C} \int_0^t i_{as} dt \quad (3)$$

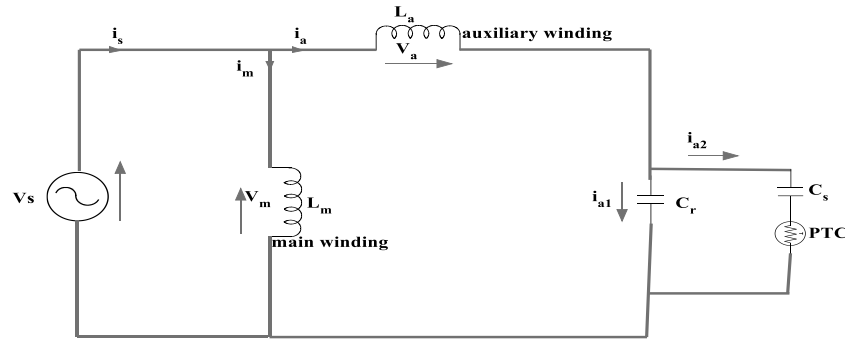


Figure 1. Circuit diagram of a single-phase interior permanent magnet synchronous motor

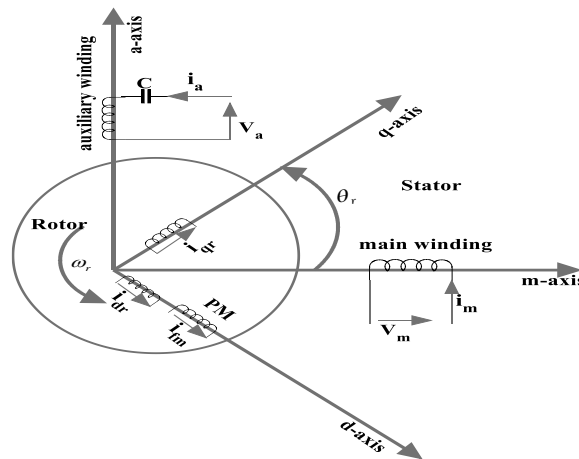


Figure 2. d-q axis model of single-phase IPMSM

The d and q axes are used to denote magnetic axes of the rotor of a synchronous machine. This is because; the two axes have been associated with the physical structure of the rotor and quite independent of any transformation. Therefore, the rotor voltage equations are written as:

$$v_{ar} = r_r i_{ar} + p \lambda_{ar} \quad (4)$$

$$v_{br} = r_r i_{br} + p \lambda_{br} \quad (5)$$

where r_r is the rotor resistance, i_{ar} and i_{br} are the rotor currents. The flux linkage equations can be written as:

$$\lambda_{ms} = L_{ms} i_{ms} + L_{msas} i_{as} + L_{msar} i_{ar} + L_{msbr} i_{br} \quad (6)$$

$$\lambda_{as} = L_{asms} i_{ms} + L_{as} i_{as} + L_{asar} i_{ar} + L_{asbr} i_{br} \quad (7)$$

$$\lambda_{ar} = L_{arms} i_{ms} + L_{aras} i_{as} + L_{ar} i_{ar} + L_{arbr} i_{br} \quad (8)$$

$$\lambda_{br} = L_{brms} i_{ms} + L_{bras} i_{as} + L_{brar} i_{ar} + L_{br} i_{br} \quad (9)$$

where L_{ms} is stator main winding self-inductance, L_{msas} denotes inductance between main and auxiliary winding, L_{msar} is the inductance between the main winding and the rotor ar axis, L_{msbr} represents inductance between the main winding and rotor br axis, L_{as} is the self-inductance of the stator auxiliary winding, L_{ar} is rotor ar axis self-inductance, L_{br} is rotor br axis self-inductance. It should be noted that the field winding on the rotor has been replaced with PM. Therefore, the flux linkage due to PM shall be introduced after transforming the flux linkage (6) to (9) to the rotor frame. It is much easier to analyse SPIPMSM by transforming voltage and flux linkage equations into the direct and quadrature reference frame. The transformation equation is given as:

$$\begin{bmatrix} f_q \\ f_d \end{bmatrix} = \begin{bmatrix} \cos\theta_r & \sin\theta_r \\ \sin\theta_r & -\cos\theta_r \end{bmatrix} \begin{bmatrix} f_m \\ f_a \end{bmatrix} \quad (10)$$

f_d and f_q are transformed quantities. It may be voltage, current or flux linkage while f_m and f_a are the main and auxiliary quantities, θ_r is the rotor angle. The d-q voltage equations are obtained by applying two-phase transformation on (1), (2), (4), and (5) as:

$$v_{qs} = R_{qs}i_{qs} + R_{qd}i_{ds} + p\lambda_{qs} + \omega_r\lambda_{ds} + v_{qc} \quad (11)$$

$$v_{ds} = R_{ds}i_{ds} + R_{dq}i_{qs} + p\lambda_{ds} - \omega_r\lambda_{qs} + v_{dc} \quad (12)$$

$$v_{qr} = 0 = r_{qr}i_{qr} + p\lambda_{qr} \quad (13)$$

$$v_{dr} = 0 = r_{dr}i_{dr} + p\lambda_{dr} \quad (14)$$

$$pv_{qc} = -\omega_r v_{dc} + \frac{1}{2C}(i_{qs} - i_{ds}\sin 2\theta_r - i_{qs}\cos 2\theta_r) \quad (15)$$

$$pv_{dc} = \omega_r v_{qc} + \frac{1}{2C}(i_{ds} - i_{qs}\sin 2\theta_r + i_{ds}\cos 2\theta_r) \quad (16)$$

where

$$R_{qs} = \frac{1}{2}[(r_m + r_a) + (r_m - r_a)\cos 2\theta_r] \quad (17)$$

$$R_{ds} = \frac{1}{2}[(r_m + r_a) - (r_m - r_a)\cos 2\theta_r] \quad (18)$$

$$R_{qd} = R_{dq} = \frac{1}{2}(r_m - r_a)\sin 2\theta_r \quad (19)$$

the quantities with subscript ds and qs are stator d- and q-axes quantities and subscript dr and qr are rotor d- and q-axes quantities. The flux linkages in d-q axis are written as;

$$\lambda_{qs} = L_{qs}i_{qs} + L_{mq}i_{qr} \quad (20)$$

$$\lambda_{ds} = L_{ds}i_{ds} + L_{md}i_{dr} + \lambda_{fm} \quad (21)$$

$$\lambda_{qr} = L_{qr}i_{qr} + L_{mq}i_{qs} \quad (22)$$

$$\lambda_{dr} = L_{dr}i_{dr} + L_{md}i_{ds} + \lambda_{fm} \quad (23)$$

the d-q current equations can be deduced from (20) to (23). λ_{fm} is PM flux linkage. The electromagnetic torque is given as;

$$T_{elect} = \frac{P}{2}(\lambda_{ds}i_{qs} - \lambda_{qs}i_{ds}) \quad (24)$$

the dynamic equation is written as:

$$p\omega_r = \frac{P}{2J}(T_{elect} - T_L) \quad (25)$$

T_L is the load torque. The rotor angular speed is given as the derivative of its angular position:

$$\omega_r = p\theta_r \quad (26)$$

P is the number of pole and p is the derivative of the quantity that as shown in.

2.2. Steady-state analysis

SPIPMSM takes time difference by capacitance and spatial phase difference of the main and auxiliary windings [32], [33]. Therefore, SPIPMSM can be considered as a two-phase motor having main winding phase and auxiliary phase. Let the ratio of the positive sequence air-gap emf E_1 to the positive

sequence stator current I_1 be defined as Z_1 (positive sequence impedance). Also, the ratio of the negative sequence air-gap emf E_2 to the negative sequence stator current I_1 be defined as Z_2 (negative sequence impedance). By definition,

$$E_1 = Z_1 I_1 \quad (27)$$

$$E_2 = Z_2 I_2 \quad (28)$$

the symmetrical components of the applied voltage, V_1 and V_2 , to the stator windings, all windings referred to the main winding, is given by:

$$\begin{bmatrix} V_1 \\ V_2 \end{bmatrix} = \begin{bmatrix} 1 & -j/K \\ 1 & j/K \end{bmatrix} \begin{bmatrix} V_m \\ V_a \end{bmatrix} \text{ or } \begin{bmatrix} V_m \\ V_a \end{bmatrix} = \begin{bmatrix} 1 & 1 \\ jK & -jK \end{bmatrix} \begin{bmatrix} V_1 \\ V_2 \end{bmatrix} \quad (29)$$

also, to find the symmetrical component currents. The circuit diagrams for two phases of SPIPMSM are as shown in Figure 3. Figure 3(a) shows the main winding phase while Figure 3(b) shows the auxiliary winding phase.

$$\begin{bmatrix} I_1 \\ I_2 \end{bmatrix} = \begin{bmatrix} 1 & -jK \\ 1 & jK \end{bmatrix} \begin{bmatrix} I_m \\ I_a \end{bmatrix} \text{ or } \begin{bmatrix} I_m \\ I_a \end{bmatrix} = \begin{bmatrix} 1 & 1 \\ j/K & -j/K \end{bmatrix} \begin{bmatrix} I_1 \\ I_2 \end{bmatrix} \quad (30)$$

$$V_m = I_m Z_{lm} + E_m \quad (31)$$

$$V_a = I_a (Z_{la} + Z_c) + E_a \quad (32)$$

applying transformation of (29) on (31) and (32) gives:

$$V_m = I_m Z_{lm} + \frac{1}{\sqrt{2}} (E_1 + E_2) \quad (33)$$

$$V_a = I_a (Z_{la} + Z_c) + \frac{jK}{\sqrt{2}} (E_1 - E_2) \quad (34)$$

substituting (27) and (28) in (33) and (34) gives;

$$\sqrt{2} V_m = I_1 (Z_{lm} + Z_1) + I_2 (Z_{lm} + Z_2) \quad (35)$$

$$-j\sqrt{2} \frac{V_a}{K} = I_1 \left(\frac{Z_{la} + Z_c}{K^2} + Z_1 \right) - I_2 \left(\frac{Z_{la} + Z_c}{K^2} + Z_2 \right) \quad (36)$$

taking the sum and the difference of (35) and (36) gives;

$$V_1 = I_1 \left(\frac{Z_{la} + Z_c}{2K^2} + \frac{Z_{lm}}{2} + Z_1 \right) - I_2 \left(\frac{Z_{la} + Z_c}{2K^2} - \frac{Z_{lm}}{2} \right) \quad (37)$$

$$V_2 = I_2 \left(\frac{Z_{la} + Z_c}{2K^2} + \frac{Z_{lm}}{2} + Z_2 \right) - I_1 \left(\frac{Z_{la} + Z_c}{2K^2} - \frac{Z_{lm}}{2} \right) \quad (38)$$

In (37) and (38) can be used to draw the equivalent circuit diagram of SPIPMSM as shown in Figure 4. The phasor diagram of SPIPMSM drawn from the equivalent circuit is shown in Figure 5. The negative sequence produces backward revolving field at double frequency. This double frequency backward revolving field generates heat and causes pulsation in the electromagnetic torque developed and degrades the performance of the motor. The negative torque must be minimized by letting the negative sequence current tends to zero. This can be achieved by proper selection of run capacitor and turn ratio value. So, setting the negative sequence current to zero in (37) and (38):

$$(Z_{lm} + Z_1) = jK \left(\frac{Z_{la} + Z_c}{K^2} + Z_1 \right) \quad (39)$$

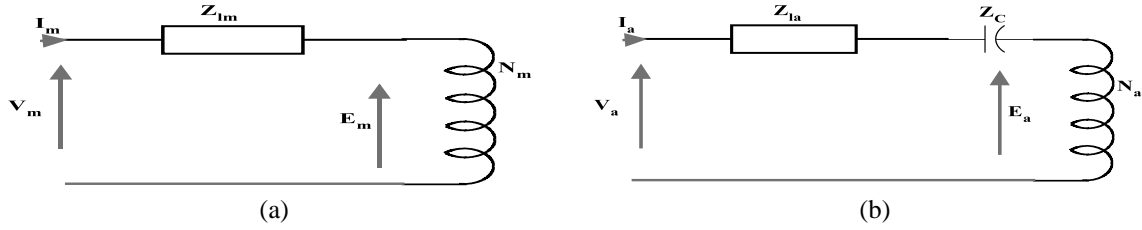


Figure 3. Two phases of SPIPMSM (a) main phase winding and (b) auxiliary phase winding circuit connections

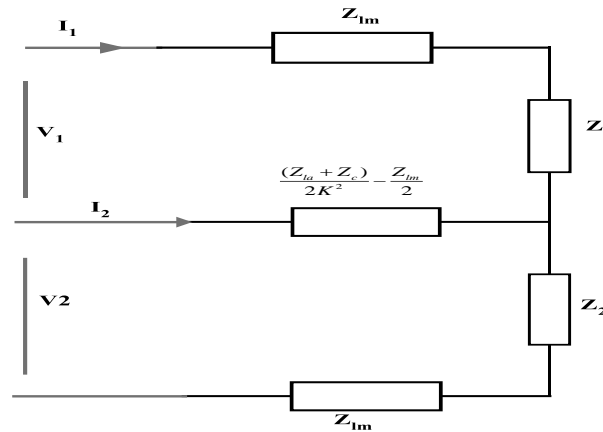


Figure 4. Equivalent circuit diagram of SPIPMSM

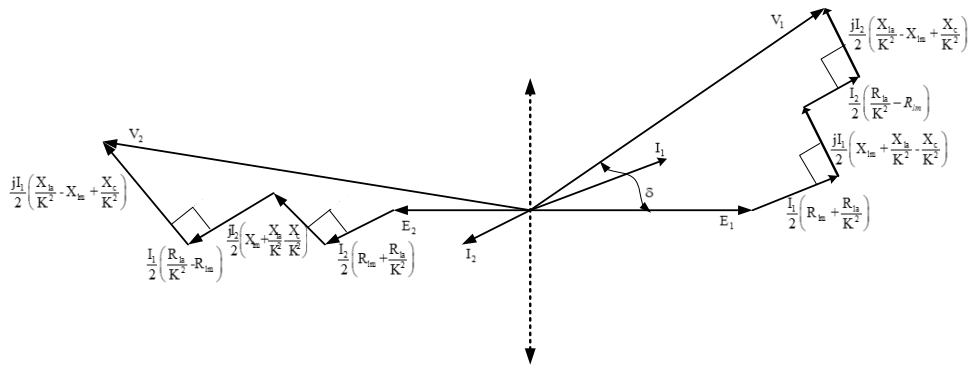


Figure 5. Phasor diagram of SPIPMSM

By equating the real and imaginary parts of the expression in (39),

$$X_C = K^2 X_1 + X_{la} + K(R_m + R_1) \tag{40}$$

the capacitor run value can be estimated from (40), where R_1 and X_1 are the positive sequence resistance and reactance respectively, K is the turn ratio of main winding to auxiliary winding, X_{la} and R_m are the main winding reactance and resistance, f is frequency of the supply voltage.

$$C_{run} = \frac{1}{2\pi f [K^2 X_1 + X_{la} + K(R_m + R_1)]} \tag{41}$$

The positive sequence system involves a forward rotating field distribution synchronized with the rotor; therefore, it is convenient to solve the vector diagram of the positive sequence air-gap voltage and current in d-q axes as presented in [33]. It should be however be noted that SPIPMSM has inverse saliency

and hence the vector axes inverted. The positive sequence impedance can be obtained by resolving the phasor diagram in Figure 6.

$$I_1 = I_{q1} - jI_{d1} \quad (42)$$

$$E_1 = E_0 + I_{d1}X_{md} + jI_{q1}X_{mq} \quad (43)$$

$$E_0 + I_{d1}X_{md} = I_{q1}X_{mq} \cot \delta \quad (44)$$

$$Z_1 = \frac{E_1}{I_1} = \frac{E_0 + I_{d1}X_{md} + jI_{q1}X_{mq}}{I_{q1} - jI_{d1}} \quad (45)$$

$$Z_1 = \frac{I_{q1}X_{mq} \cot \delta + jI_{q1}X_{mq}}{I_{q1} - jI_{d1}} \quad (46)$$

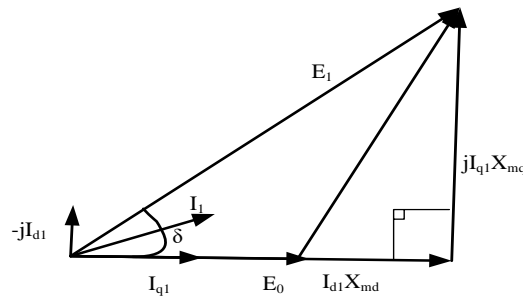


Figure 6. Vector diagram of positive sequence air-gap voltage and current in d-q rotor reference frame

If the excitation voltage is absent as in [33], then, the torque dependent expression for the machine impedance should match with the impedance of capacitor reluctance motor. Apply this assumption to (44), then, substitute for I_{d1} from (44) into (46) gives:

$$Z_1 = \frac{X_{mq} + jX_{mq} \tan \delta}{X_{md} \tan \delta - jX_{mq}} \quad (47)$$

manipulating the numerator and denominator of (47) gives:

$$Z_1 = jX_{mq} + \frac{1}{\frac{1}{j(X_{md} - X_{mq})} + \frac{X_{md} \tan \delta}{X_{mq}(X_{md} - X_{mq})}} \quad (48)$$

$$Z_1 = \frac{jX_{mq}(X_{mq} + jX_{md} \tan \delta) + jX_{mq}(X_{md} - X_{mq})}{X_{mq} + jX_{md} \tan \delta} \quad (49)$$

rationalizing (49) and re-arranging gives the positive sequence impedance in terms of the load angle.

$$Z_1 = \frac{X_{md}X_{mq} \tan \delta (X_{md} - X_{mq})}{X_{mq}^2 + X_{md}^2 \tan^2 \delta} + j \frac{X_{md}X_{mq} (X_{md} \tan^2 \delta + X_{mq})}{X_{mq}^2 + X_{md}^2 \tan^2 \delta} \quad (50)$$

The negative sequence impedance can be calculated as the average value of the apparent rotor impedances of d- and q-axes for slip of 2 [32]. R_{rd} and R_{rq} are d and q rotor resistance respectively. X_{lrq} and X_{lrq} are d and q-axis rotor leakage reactance.

$$Z_2 = \frac{1}{2} \left(\frac{jX_{md} \left(\frac{R_{rd}}{2} + jX_{lrq} \right)}{\frac{R_{rd}}{2} + j(X_{md} + X_{lrq})} + \frac{jX_{mq} \left(\frac{R_{rq}}{2} + jX_{lrq} \right)}{\frac{R_{rq}}{2} + j(X_{mq} + X_{lrq})} \right) \quad (51)$$

The equivalent circuit presented in Figure 4 can now be re-drawn as in Figure 7. Since the positive sequence current contributes to the synchronous action at steady state and negative sequence contribute to induction action at starting, then, the circuit of Figure 7 can be modified as in Figure 8. I_0 and I_L are magnetizing current and load current respectively.

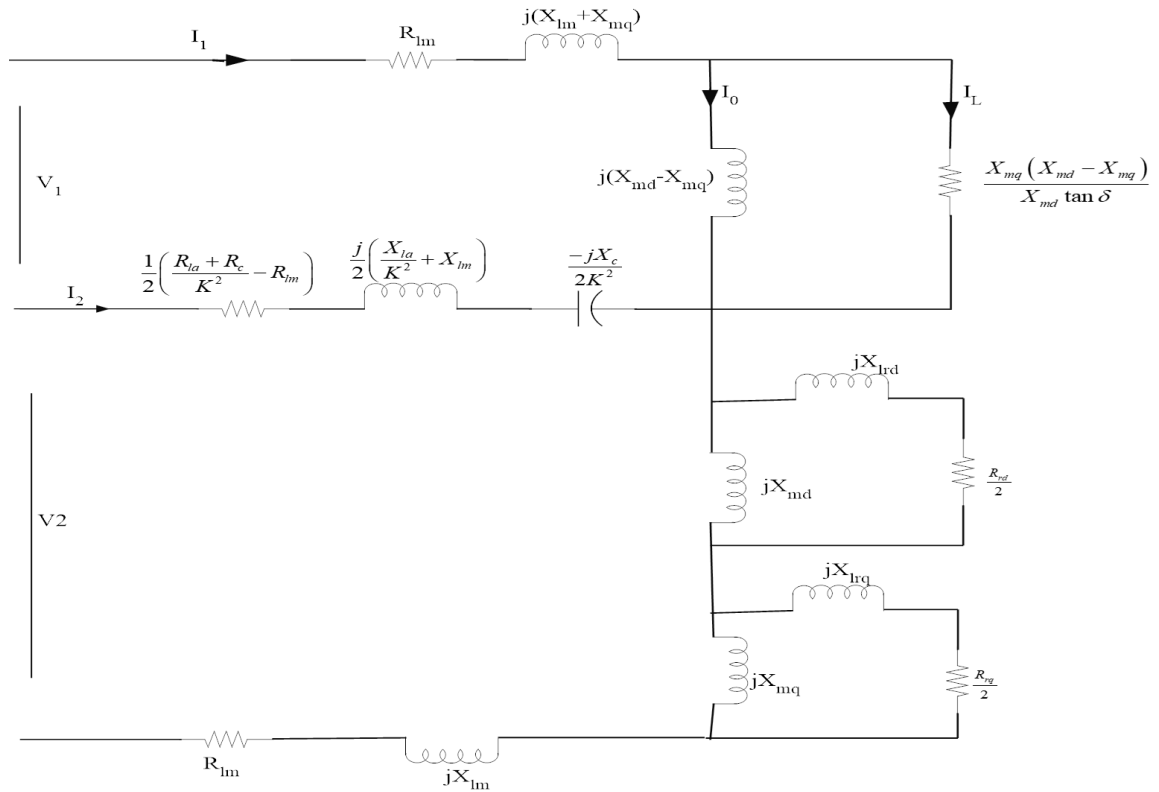


Figure 7. Equivalent circuit diagram of SPIPMSM

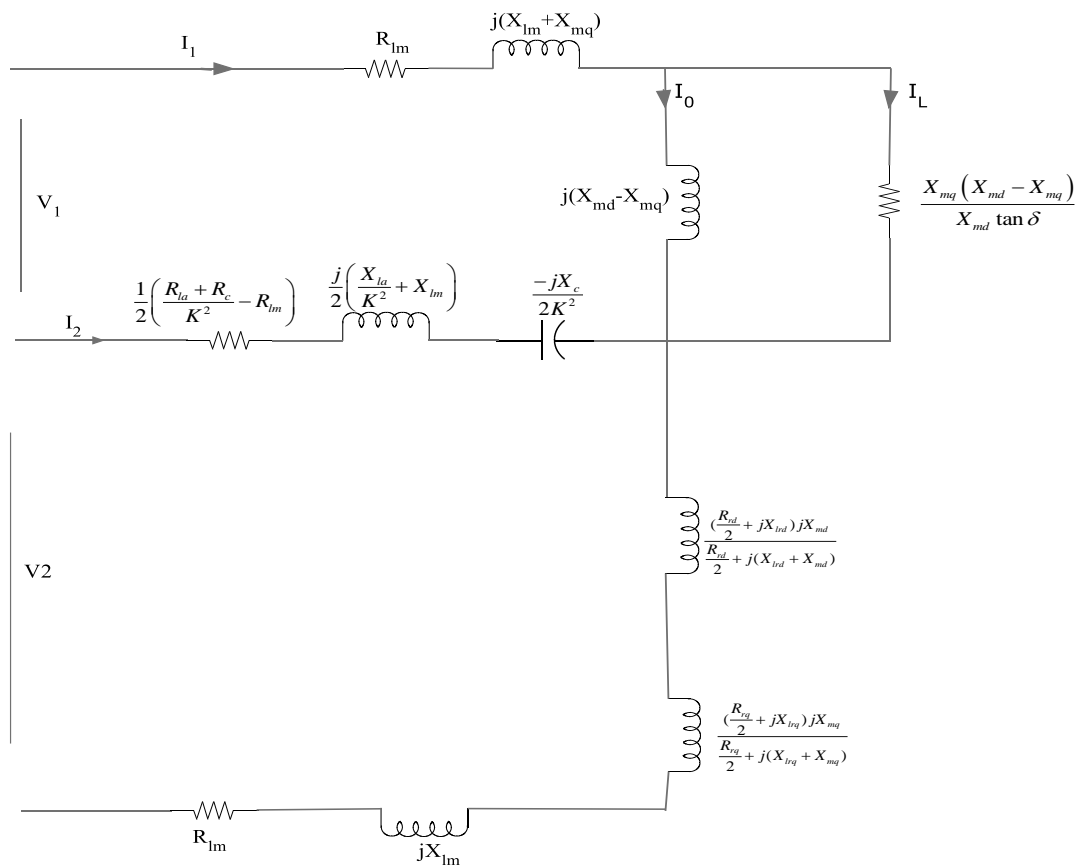


Figure 8. Modified equivalent circuit of SPIPMSM

The laboratory set up to measure the dynamic behavior of the prototype motor developed is as shown in Figure 9. The developed SPIPMSM was connected to the DC machine via the torque sensor. The shafts of the torque sensor were connected to the shafts of the test motor and the DC generator by using single membrane coupling, so as to provide a torsional rigidity. The input voltage was supplied to the stator of SPIPMSM in steps up to the rated voltage from a variable transformer. A variable resistive load was connected to the DC machine which acted as a generator. The torque sensor was used to measure the dynamic torque and speed of the test motor. The torque sensor was connected to a personal computer (PC) via universal serial bus (USB) and its output displayed and recorded using TorqView. TorqView is a virtual instrumentation display PC interface software program for use with the torque sensor. The torque sensor was powered by a supply voltage of 12 to 32 vanguard direct current (VDC) with minimum current of 1amp. In order to perform the load test, the DC generator was provided with a field current of 0.8 A. The dynamic torque and speed of the motor were measured at each time the variable resistive load on the DC motor was increased. The dynamic simulation of a ½ hp 4 poles SPIPMSM was carried out using embedded MATLAB and the results of the simulation result was compared with the experimental result.

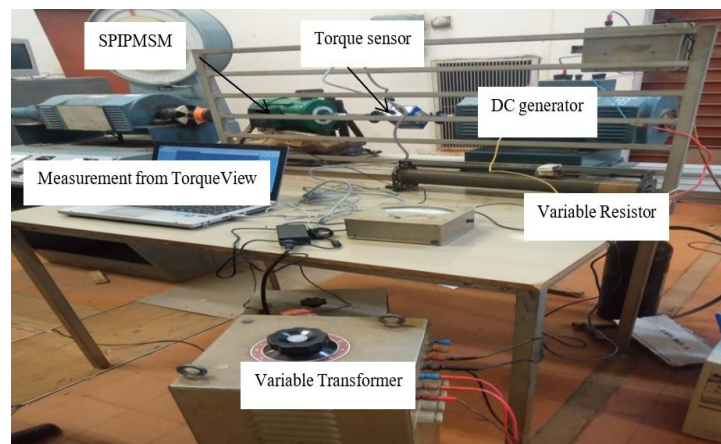


Figure 9. Image of the experimental setup for SPIPMSM

3. RESULTS AND DISCUSSION

The results obtained when a ½ hp, 4 poles SPIPMSM motor was simulated for dynamic analysis are presented. Figure 10 shows the developed electromagnetic torque when a load of 1 N was added after the step time of 2 seconds. Synchronism was attained at about 0.5 second as seen in Figure 10; the developed torque has a value of about 1.5 Nm at no load and about 2.3 Nm when loaded after 2 seconds. Figure 11 compares the experimental and simulation torque-speed plots. The two plots compared favourably. The main winding current of SPIPMSM is shown in Figure 12 while the auxiliary current is shown in Figure 13.

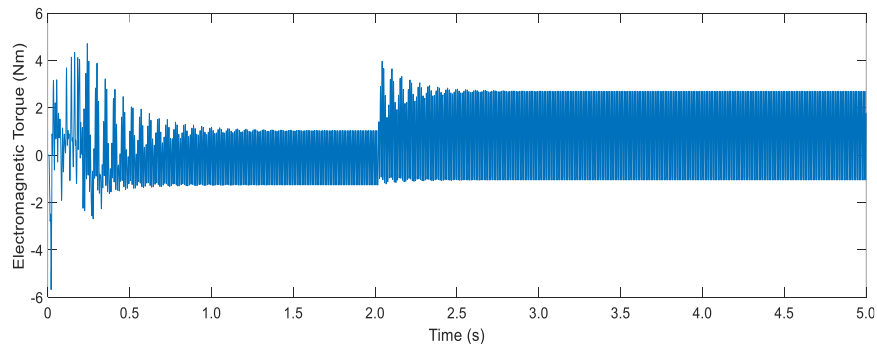


Figure 10. Electromagnetic torque versus time response of SPIPMSM

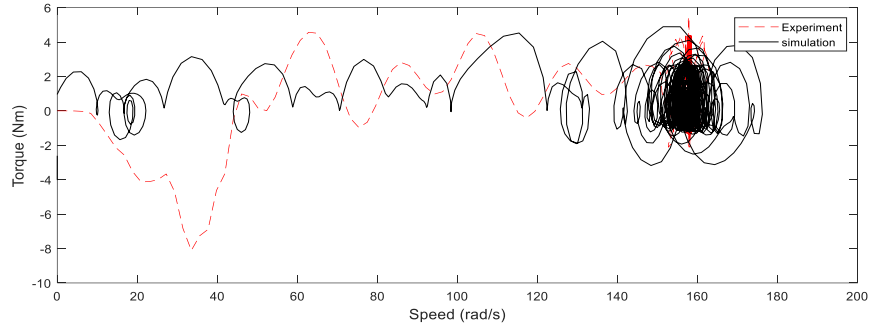


Figure 11. Experimental and simulation torque-speed characteristics of SPIPMSM

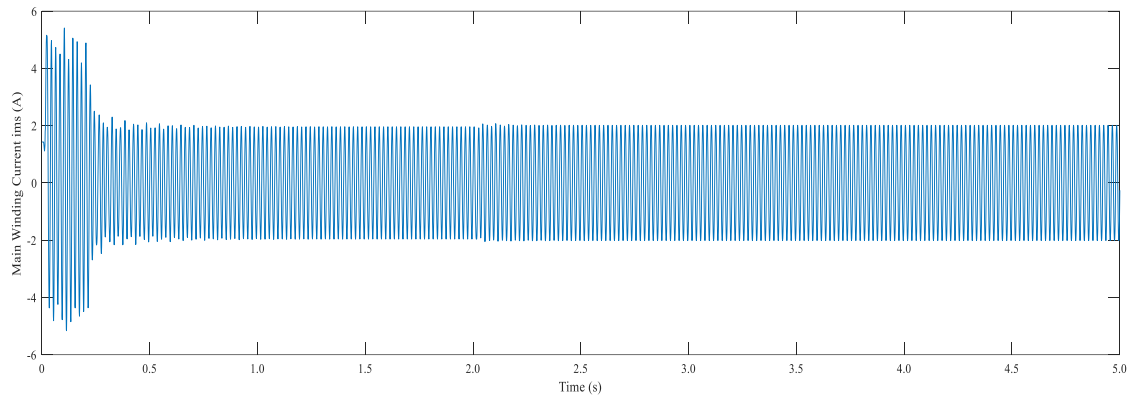


Figure 12. Stator main winding current

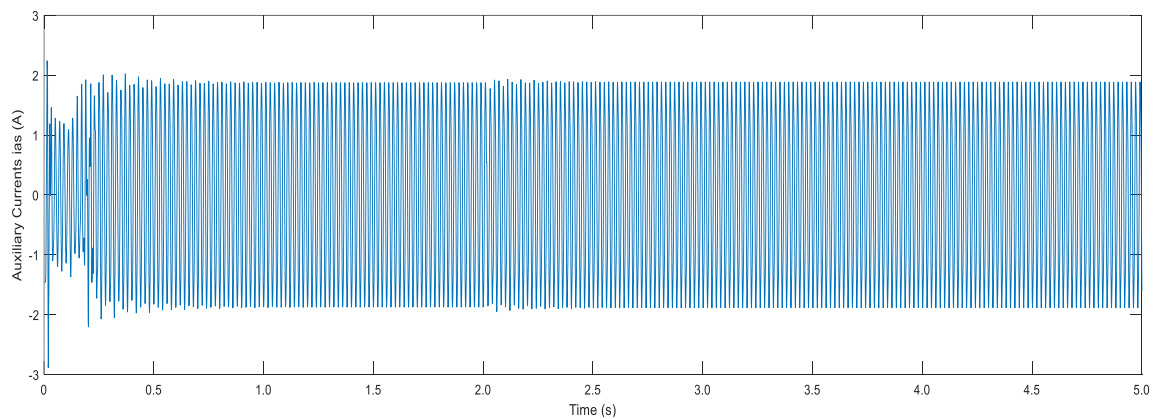


Figure 13. Stator auxiliary current

The steady state performance analysis of single-phase interior permanent magnet synchronous motor of 1 kW ratings was carried out using symmetrical components method. The simulation was carried out using m-file in MATLAB. The results are as presented from Figures 14 to 17. In Figure 14, the positive sequence, negative sequence, auxiliary and main currents are presented. It can be observed that the positive sequence current is higher in value than the negative sequence current. This implies that at steady state, the positive sequence current is required for the synchronous motor action of the machine. The negative sequence, positive sequence and main currents respectively increase with increase in the rotor angle positions. However, the negative sequence current did not increase significantly like the positive sequence and main phase current. Figure 14 equally agrees with the theoretical model of the motor. The auxiliary current magnitude remains almost constant. Rotor current behaves like the negative sequence and it could also be observed that the main current grows gradually to maximum.

Figure 17 shows the negative sequence torque is almost going down to zero. The positive sequence and total torque behave alike at steady state. It can also be observed that the maximum value of torque for maximum power is 3.20 Nm, 1.2 rad (68.75°) of rotor angle. It can be observed the negative sequence power is almost going down to zero as well. The positive sequence and total power behave alike at steady state in the same manner with the torque characteristics. The maximum power that can be achieved is 1000 watts, 1.2 rad (68.75°) of rotor angle.

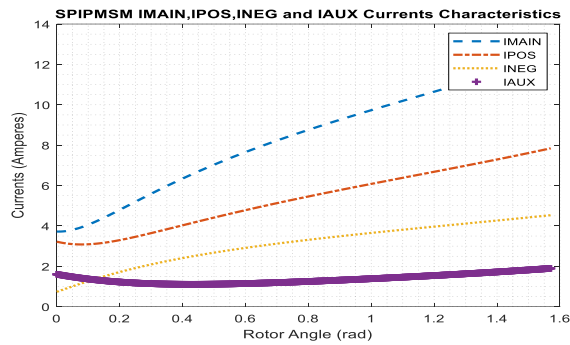


Figure 14. Currents characteristics of SPIPMSM

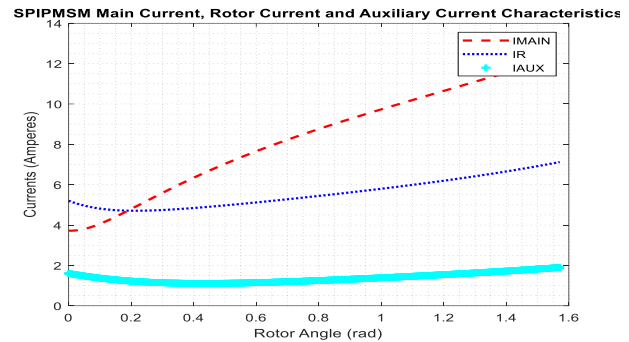


Figure 15. Main, rotor, and auxiliary currents characteristics

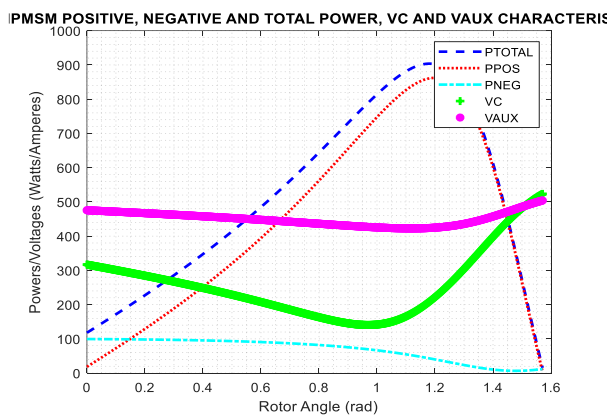


Figure 16. Positive sequence power, negative sequence power, total power, capacitor voltage and auxiliary voltage characteristics

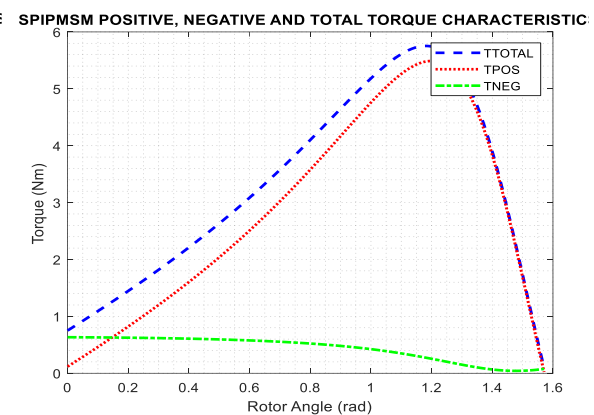


Figure 17. Positive sequence, negative sequence, and total torque characteristics

4. CONCLUSION

The dynamic and steady-state performance analysis of single-phase interior permanent magnet synchronous motor has been carried out. The results obtained were in agreement with the theoretical analysis. The motor attained synchronism at about 0.5 seconds when loaded with a load torque of 1 N-m. The motor developed torque of 1.5 Nm at no-load and 2.3 Nm at load. This shows that the motor responded better to the added load. The experimental and simulation torque speed characteristics behave in the same manner. The simulation and the experimental torque speed synchronized at exactly synchronous speed. Also, at steady state, the positive sequence current is higher than the negative sequence of SPIPMSM. This shows that the positive sequence current is more required for synchronism at steady-state. This observation was also affirmed by the phasor diagram. The magnitude of the positive sequence of the phasor diagram increases, while the negative sequence remains almost constant. Infact, the negative sequence current causes the heating-up of the motor at steady-state. It is required that the negative sequence current be minimized at steady-state. This is achieved by proper selection of the running capacitor at balance operation of the motor.




REFERENCES

- [1] R. J Kerkman, "Machine Analysis with Unbalanced Terminal Constraints by d-q Harmonic Balance," *IEE Proceedings B-Electric Power Applications*, vol. 128, no 6, pp. 343–357, 1981.
- [2] J. F. Gieras, "Permanent Magnet Motor Technology Design and Applications," CRC press, 2009.
- [3] A. Alidousti, A. Sadoughi, H. Behbahani, and Y. Raiesi, "A new rotor prototype for single phase line start permanent magnet synchronous motor based on amendments to a small industrial shaded pole induction motor," *2018 9th Annual Power Electronics, Drives Systems and Technologies Conference (PEDSTC)*, 2018, pp. 218–223, doi: 10.1109/PEDSTC.2018.8343799.
- [4] M. A. Rahman *et al.*, "Advances on Single-Phase Line-Start High Efficiency Interior Permanent Magnet Motors," in *IEEE Transactions on Industrial Electronics*, vol. 59, no. 3, pp. 1333–1345, March 2012, doi: 10.1109/TIE.2011.2167111.
- [5] T. J. E. Miller, "Single-Phase Permanent-Magnet Motor Analysis," in *IEEE Transactions on Industry Applications*, vol. IA-21, no. 3, pp. 651–658, May 1985, doi: 10.1109/TIA.1985.349722.
- [6] P. Sethupathi and N. Senthilnathan "Comparative analysis of line-start permanent magnet synchronous motor and squirrel cage induction motor under customary power quality indices" *Journal of Electrical Engineering*, vol. 102, no. 3, pp. 1339–1349, February 2020, doi: 10.1007/s00202-020-00955-2.
- [7] T. J. E. Miller, M. Popescu, C. Cossar, M. McGilp, and J. A. Walker, "Calculating the interior permanent-magnet motor," *IEEE International Electric Machines and Drives Conference, 2003. IEMDC'03.*, vol. 2, pp. 1181–1187, 2003, doi: 10.1109/IEMDC.2003.1210390.
- [8] K. Dambrauskas, J. Vanagas, T. Zimnickas, A. Kalvaitis, and M. Azubalis, "A method for efficiency determination of permanent magnet synchronous motor," *Energies*, vol. 13, no. 4, p. 1004, February 2020, doi: 10.3390/en13041004.
- [9] J. Singh, B. Singh, S. P. Singh, and M. Naim, "Investigation of performance parameters of PMSM drives using DTC-SVPWM technique," *2012 Students Conference on Engineering and Systems*, 2012, pp. 1–6, doi: 10.1109/SCES.2012.6199092.
- [10] A. Yassin, M. Badr, and S. Wahsh, "Cuckoo Search Based DTC of PMSM," *International Journal of Power Electronics and Drive System (IJPEDS)*, vol. 9, no. 3, pp. 1106–1115, September 2018, doi: 10.11591/ijpeds.v9.i3.pp1106-1115.
- [11] M. Popescu, T. J. E. Miller, M. I. McGilp, G. Strappazon, N. Trivillin, and R. Santarossa, "Line-start permanent-magnet motor: single-phase starting performance analysis," in *IEEE Transactions on Industry Applications*, vol. 39, no. 4, pp. 1021–1030, July–August 2003, doi: 10.1109/TIA.2003.813745.
- [12] M. Popescu, T. J. E. Miller, M. McGilp, G. Strappazon, N. Trivillin, and R. Santarossa, "Asynchronous performance analysis of a single-phase capacitor-start, capacitor-run permanent magnet motor," in *IEEE Transactions on Energy Conversion*, vol. 20, no. 1, pp. 142–150, March 2005, doi: 10.1109/TEC.2004.837307.
- [13] J. Shang, W. Tang, and C. Liu, "Optimization of Electromagnetic Performance of Single-Phase Line-Start Permanent Magnet Synchronous Motor Based on the Finite Element Method," *2019 22nd International Conference on Electrical Machines and Systems (ICEMS)*, 2019, pp. 1–6, doi: 10.1109/ICEMS.2019.8922439.
- [14] J. W. Finch and P. J. Lawrenson, "Asynchronous Performance of Single-Phase Reluctance Motors," *Proceedings of the Institution of Electrical Engineers*, vol. 126, no 12, pp. 1248–1254, December 1979, doi: 10.1049/piee.1979.0217.
- [15] E. C. Lovelace, T. M. Jahns, and J. H. Lang, "A saturating lumped-parameter model for an interior PM synchronous machine," in *IEEE Transactions on Industry Applications*, vol. 38, no. 3, pp. 645–650, May–June 2002, doi: 10.1109/TIA.2002.1003413.
- [16] L. Anh-Tuan, B. Duc-Hung, and P. Anh-Tuan, "Saturable q-axis magnetizing inductance calculation of Line Start-Permanent Magnet Synchronous Motors using Lumped Parameter Mode," *2016 IEEE International Conference on Sustainable Energy Technologies (ICSET)*, 2016, pp. 364–368, doi: 10.1109/ICSET.2016.7811811.
- [17] K. Bensaida, I. Abdennadher, A. Masmoudi, and F. Marignetti, "On the enhancement of the starting capabilities of single phase line-start PMSMs," *2018 Thirteenth International Conference on Ecological Vehicles and Renewable Energies (EVER)*, 2018, pp. 1–6, doi: 10.1109/EVER.2018.8362335.
- [18] D. Gope and S.K. Goel, "Design optimization of permanent magnet synchronous motor using Taguchi method and experimental validation," *International Journal of Emerging Electric Power System*, vol. 22, no. 1, pp. 9–20, December 2020, doi: 10.1515/ijeeps-2020-0169.
- [19] J. Si, S. Zhao, H. Feng, R. Cao, and Y. Hu, "Multi-objective optimization of surface-mounted and interior permanent magnet synchronous motor based on Taguchi method and response surface method," in *Chinese Journal of Electrical Engineering*, vol. 4, no. 1, pp. 67–73, March 2018, doi: 10.23919/CJEE.2018.8327373.
- [20] D. Uğur and M. A. Caner, "Using Taguchi method in defining critical rotor pole data of LSPMSM considering the power factor and efficiency," *Tehnicki Vjesnik*, vol. 24, no. 2, pp. 347–353, 2017, doi: 10.17559/tv-20140714225453.
- [21] Y. Li, Y. Kang, T. Wang, L. Guo, H. Wang, and H. Wang, "Dynamic characteristics research on single phase permanent magnet swing angle torque motor of high voltage vacuum circuit breaker," *2017 IEEE Transportation Electrification Conference and Expo, Asia-Pacific (ITEC Asia-Pacific)*, 2017, pp. 1–5, doi: 10.1109/ITEC-AP.2017.8081009.
- [22] R. Manko *et al.*, "Design of experiment in optimization of permanent magnet synchronous motor performance," *2017 International Conference on Modern Electrical and Energy Systems (MEES)*, 2017, pp. 36–39, doi: 10.1109/MEES.2017.8248932.
- [23] K. Kurihara, H. Fukuda, and T. Kubota, "Trade-off with starting capability to maximize efficiency of a single-phase line-start permanent magnet motor," *2017 20th International Conference on Electrical Machines and Systems (ICEMS)*, 2017, pp. 1–4, doi: 10.1109/ICEMS.2017.8056122.
- [24] S. Kahourzade, W. L. Soong, and P. Lillington, "Single-Phase Loading Behavior of the Isolated 3ph Spoke Interior Permanent-Magnet Generator," in *IEEE Transactions on Industry Applications*, vol. 53, no. 3, pp. 1860–1869, May–June 2017, doi: 10.1109/TIA.2016.2645508.
- [25] S. S. Apeshi, E. S. Obe, and J. E. Akpama, "Performance Analysis of Single Phase Interior Permanent Magnet Synchronous Generator," *Nigerian Journal of Technology (NIJOTECH)*, vol. 38, no. 4, pp. 980–986, 2019, doi: 10.4314/njt.v38i4.22.
- [26] Y. AKYÜN, H. NORRY, M. Z. TALAS, and H. KÜRÜM, "Design Analysis and Verification of PMSM Motor for Dishwasher Machine," *2019 4th International Conference on Power Electronics and their Applications (ICPEA)*, 2019, pp. 1–7, doi: 10.1109/ICPEA1.2019.8911146.
- [27] D. Y. Um and G. S. Park, "Determination Scheme of Stator Parameters for Making Rotating Fields Circular in a Single-Phase Induction Motor," in *IEEE Transactions on Magnetics*, vol. 56, no. 1, pp. 1–5, January 2020, doi: 10.1109/TMAG.2019.2949031.
- [28] U. Sharma and B. Singh, "Suitability Estimation of Ceiling Fan SPIMs Using Locked Rotor and No Load Tests Assisted With FEA," *2020 IEEE International Conference on Power Electronics, Smart Grid and Renewable Energy (PESGRE2020)*, 2020, pp. 1–6, doi: 10.1109/PESGRE45664.2020.9070716.
- [29] H. Saneie and Z. Nasiri-Gheidari, "Performance Analysis of Outer-Rotor Single-Phase Induction Motor Based on Magnetic Equivalent Circuit," in *IEEE Transactions on Industrial Electronics*, vol. 68, no. 2, pp. 1046–1054, February 2021, doi: 10.1109/TIE.2020.2969125.
- [30] U. Sharma and B. Singh, "Robust design methodology for single phase induction motor ceiling fan," *IET Electric Power Applications*, vol. 14, no. 10, pp. 1846–1855, July 2020, doi: 10.1049/iet-epa.2020.0017.




- [31] D. W. Olive and G. Richards, "Asynchronous Operation of A. C. Synchronous Machines the Linear Equivalent Circuit," in *IEEE Transactions on Power Apparatus and Systems*, vol. PAS-97, no. 5, pp. 1627–1636, September 1978, doi: 10.1109/TPAS.1978.354654.
- [32] S. S. L. Chang, "An Analysis or Unexcited Synchronous Capacitor Motors," in *Transactions of the American Institute of Electrical Engineers*, vol. 70, no. 2, pp. 1978–1982, July 1951, doi: 10.1109/T-AIEE.1951.5060660.
- [33] B. N. Chaudhari and B. G. Fernandes, "Equivalent circuit of single phase permanent magnet synchronous motor," *2001 IEEE Power Engineering Society Winter Meeting. Conference Proceedings (Cat. No.01CH37194)*, vol. 3, pp. 1378–1381, 2001, doi: 10.1109/PESW.2001.917291.

BIOGRAPHIES OF AUTHORS



Benjamin Olabisi Akinloye    was born in Ogbomoso, Oyo State Nigeria in 1984. He received B. Tech from Ladoke Akintola University of Technology, Ogbomoso, Oyo State, Nigeria and M.Eng degree from Federal University of Technology, Akure, both in 2009 and 2014 respectively. He is currently working towards his Ph.D degree in the department of Electrical Engineering, University of Nigeria, Nsukka, Nigeria. He is presently a Lecturer in the Department of Electrical and Electronic Engineering, Federal University of Petroleum Resources, Effurun, Nigeria. His research interests include power system analysis and electrical machine analysis. He can be contacted at email: akinloye.benjamin@fupre.edu.ng.



Emeka Simon Obe    was born in Uda Enugu Ezike, Nigeria. He received his B. Engineering, M. Engineering and Ph.D. degrees in Electrical Engineering from University of Nigeria in 1994, 1999 and 2002, respectively. Since 1999 he has been with the Department of Electrical Engineering, University of Nigeria, Nsukka where he is currently a professor. Obe has been a visiting researcher at Tennessee Technological University, USA in 2004 and 2006, at the University of the Ryukyus, Japan in 2005 and at Technische Universitat Darmstadt, Germany 2008-2009. He is currently the Dean, Faculty of Engineering (2020-date). Obe is an associate editor of IET electric power applications of UK, associate editor of electric power components and systems and editor-in-chief, Nigerian Journal of Technology. He is a fellow of AvH, Germany, MIEEE, MNSE, and a corporate engineer in Nigeria. His research interests are ac machine analysis, design and drives. Obe has published over 50 articles in reputable journals and high echelon conference proceedings. He can be contacted at email: simon.obe@unn.edu.ng.